ELSEVIER

Journal of Chromatography B, 732 (1999) 193–201

JOURNAL OF CHROMATOGRAPHY B

www.elsevier.com/locate/chromb

Analyzing mixtures of amino acids and carbohydrates using bi-modal integrated amperometric detection

Petr Jandik[a], Alan P. Clarke[a], Nebojsa Avdalovic[a,*], Dana C. Andersen[b], Jerry Cacia[b]

[a]*Dionex Corporation, 445 Lakeside Drive, Sunnyvale, CA 94088, USA*
[b]*Genentech Inc., One DNA Way, South San Francisco, CA 94080, USA*

Received 26 April 1999; received in revised form 14 June 1999; accepted 16 June 1999

Abstract

Described in this work is a new detection methodology – bi-modal integrated amperometric detection – for identifying peaks and as a tool for solving difficult separation problems. Bi-modal integrated amperometry makes it possible to selectively detect amino acids, amino sugars, and carbohydrates following their separation by anion-exchange. Selectivity is gained by two different methods of integrating anodic current on an otherwise identical waveform. As with the single-mode integrated amperometry reported previously, the limits of detection are in the femtomole range and linear calibration plots are possible over three orders of magnitude. This new detection method does not require analyte derivatization. The practical utility of this new technique is demonstrated in the analysis of amino acids and sugars in a recombinant mammalian cell culture medium.

Keywords: Bi-modal integrated amperometric detection; Amino acids; Carbohydrates

1. Introduction

The initial interest in electrochemical detection for HPLC was engendered by a successful application to the analysis of catecholamines in biological fluids [1]. The next important advance arrived in the form of electrochemical detection of carbohydrates after their separation by anion-exchange chromatography [2]. Whereas the older detection techniques relied primarily on carbon electrodes (e.g. glassy carbon, graphite), the newer methodology has been expanded to include metals such as gold, platinum, and silver. While the older methods are based on amperometry at a constant potential, the more recent applications utilize an optimized sequence of potentials.

The potential sequence, consisting of several potentials and cycled with a frequency usually exceeding 1 Hz, is called a waveform. Waveform potentials effect oxidation (less frequently, reduction) of analytes and removal of reaction products from the electrode. Removal of the reaction products is necessary for a good reproducibility of detection. The surface reaction of the analyte is detected by current integration over a time interval that represents only a fraction of the waveform cycle. The detection response is thus recorded in Coulombs. The term ''integrated pulsed amperometric detection'' has been introduced to describe all detection techniques based on current integration in conjunction with rapidly changed (pulsed) potentials.

Optimization of waveform potentials frequently requires non-chromatographic techniques such as

*Corresponding author.

0378-4347/99/$ – see front matter
PII: S0378-4347(99)00284-4

cyclic voltammetry with a rotated disk electrode. A recently published book [3] provides background information on cyclic voltammetry and its use in the optimization of integrated pulsed amperometry.

In an earlier paper, we described a new waveform for integrated amperometric detection of amino acids following their separation by high-pH anion-exchange chromatography [4]. Gradient separations of 18 or more amino acids are completed within a total run time of less than 50 min. The new waveform makes it possible to detect in the femtomole range (e.g. Arg 0.15, Lys 0.21, Gln 0.48 pmol detection limits as 3× noise) with a good linearity of calibration over three orders of magnitude.

Our optimized waveform represents the continuation of a development process initiated by Johnson et al. in 1981. Two reviews [5,6] summarize the progress achieved to date, and explain optimization of electrode reactions of the large number of predominantly aliphatic compounds at noble metal electrodes.

Briefly, there are two modes of anodic, electrocatalytic detection with gold and platinum electrodes. Each mode has, so far, been applied exclusively to specific categories of compounds. Thus, detection at oxide-free surfaces [Mode I, −0.6 to +0.2 V vs. Standard Calomel Electrode (SCE) for Au] is useful for hydroxylated compounds such as alcohols, glycols, monosaccharides, polysaccharides, etc., while oxide-catalyzed detection (Mode II, >+0.2 V vs. SCE for Au) has been utilized for aliphatic amines and amino acids. Although some work has been done in acidic eluates [7–10] after a cation-exchange separation, most reports describe various applications of the two modes for the detection in alkaline eluates from an anion-exchange column.

An application of this new detection methodology is demonstrated in the analysis of mammalian cell culture medium used to grow large quantities of mammalian cells [11]. The concentrations of glucose, typically the primary source of carbon, and the amino acids are critical components of media optimized for cell growth and recombinant protein production. Several recent reports have demonstrated substantial improvements in cell culture performance through the use of complex feeding strategies using glucose, glutamine, and other amino acids and nutrients [11–14]. These recent results illustrate the potential utility of straightforward techniques that can sensitively measure a range of metabolites in cell culture matrices, to be used in conjunction with recombinant cell culture.

While optimizing our new method for the analysis of cell culture media, we observed strong signals due to glucose and other compounds which are normally detected by Mode I, in Mode II of pulsed electrochemical detection (PED). We then modified the waveform to allow anodic current sampling in both modes and used it to compare the responses for the analytes of interest in fermentation broths. As described in this report, this ''Bi-Modal'' approach to PED provides useful information in the identification and quantification of different types of compounds in complicated matrices, and even aids in the distinction between and identification of co-eluting compounds.

2. Experimental

Cyclic voltammetry was performed with a potentiostat model AFCBP1 (Pine Instruments, Grove City, PA, USA). Rotation of the Au-disk electrode (d=5 mm) was controlled by a model AFMSRX Analytical Rotator (Pine Instruments). All sample solutions were thoroughly de-aired by sparging with purified nitrogen (Altair, San Ramon, CA, USA) prior to data collection. An AT-MIO-16X I/O board (National Instruments, Austin, TX, USA) in a PC was used for data acquisition.

We performed all the chromatographic experiments with a DX-500 liquid chromatograph (Dionex, Sunnyvale, CA, USA). The instrument consisted of a GP40 gradient pump equipped with an on-line degas module, LC30 column thermostat set at 30°C, and an ED40 electrochemical detector connected to a thin-layer cell. The Kel-F-embedded gold working electrode had a diameter of 1 mm. The counterelectrode consisted of a titanium cell body across the 25-μm channel formed by a gasket. As a reference electrode, we utilized a glass and Ag/AgCl combination electrode placed downstream from the gold working electrode.

The chromatographic system also consisted of a set of AminoPac PA10 prototype columns (a 250×2-mm column and a 40×2-mm guard column,

Dionex). The gradient elution was performed at a flow-rate of 0.25 ml/min with one of the three ternary gradients shown in Table 1. Mobile phase I was 18 MΩ water vacuum-filtered through a 0.2-μm nylon filter. Mobile phase II, a 250 m*M* sodium hydroxide solution, was prepared by diluting an aliquot of 50% sodium hydroxide (Fisher Scientific, Fair Lawn, NJ, USA) in the corresponding volume of 18 MΩ water filtered through a 0.2-μm nylon filter. Mobile phase III, a 1.0 *M* sodium acetate solution, was prepared by dissolving an aliquot of anhydrous sodium acetate (Fluka, Buchs, Switzerland) in 18 MΩ water and filtering the 250 m*M* solution through a 0.2-μm nylon filter. All eluents were kept under nitrogen to prevent the accumulation of atmospheric carbon dioxide. PeakNet Chromatography Software, version 5.0 (Dionex), was used for data acquisition and processing.

Table 1
Gradient conditions

Gradient	Time (min)	NaOH (m*M*)	Na Ac. (m*M*)	Curve
A				
	0.0	60		
	2.0	60		
	8.0	90		8
	11.0	90		
	18.0	50	400	8
	21.0	40	400	5
	23.0	40	700	8
	42.0	40	700	
	42.1	200		5
	44.1	200		
	44.2	60		5
	70.0	60		
B				
	0.0	60		
	7.0	60		
	17.0	60	450	8
	20.0	60	600	8
	24.0	60	600	
	24.1	200		5
	26.0	200		
	26.1	60		5
	50.0	60		
C				
	0.00	40		
	2.00	40		
	12.0	80		8
	16.0	80		
	24.0	60	400	8
	35.0	60	400	
	35.1	200		5
	37.1	200		
	37.2	40		5
	60.0	40		

The chromatographic standards were prepared by diluting Standard Reference Material 2389 (NIST, Gaithersburg, MD, USA). Corresponding aliquots of additional amino acids, amino sugars or sugars were added to SRM 2389 during the dilution step. To increase the stability of dilute standards, the dilutions were carried out with a 20-ppm sodium azide diluent. All additional standard components and sodium azide were from Sigma-Aldrich (St. Louis, MO, USA).

3. Results and discussion

3.1. Cyclic voltammetry (C.V.)

C.V. is an electroanalytical technique using a three-electrode potentiostat (see Ref. [3] for a more detailed description of C.V.). The potential is adjusted between the working electrode (i.e. gold in this report) and the reference electrode (i.e. Ag/AgCl) and cycled between two values. All three electrodes are immersed in the analyte solution. The current is measured between the working electrode and the counterelectrode. The resulting current-potential plot is called a cyclic voltammogram.

In their 1993 review, Johnson et al. [6] compared cyclic voltammograms of glycine, ethylamine, and ethanolamine. While the cyclic voltammograms of amine and amino acid are typical of anodic oxidation in Mode II, those of alkanolamine consist of a combination of Mode I and Mode II features. There are also differences between the voltammogram of the amine and the amino acid, which are most obvious between +0.1 V and +0.6 V during the positively directed portion of the scan. The voltammogram of amine exhibits a pronounced single maximum at ~+0.2 V. In contrast, the recording of the amino acid contains two maxima at ~+0.1 V and +0.3 V, respectively. On a molar basis, the response for the amino acid is lower than that of the amine.

We have generated cyclic voltammograms of 15 amino acids commonly found in protein hydrolysates

(cysteine and methionine are not included since their analysis in hydrolysates typically involves a conversion to cysteic acid and methioninesulfone, respectively) and seven additional amino acids. All the voltammograms resemble one of the three recordings from the 1993 review, and can thus be assigned to three categories.

3.1.1. Category I: Aliphatic, aromatic, and carboxylated amino acids

The main features of the voltammogram of leucine in Fig. 1A are similar not only to glycine, but to all other primary amino acids without a specific functional group (e.g. valine, isoleucine, and norleucine). The leucine-like appearance is also typical for some aromatic amino acids such as phenylalanine and tyrosine. The simple carboxylated amino acids (aspartic and glutamic) also fall into the same category.

3.1.2. Category II: Basic amino acids

The ''alkylamine-like'' appearance of lysine in Fig. 1B is typical for its homologues such as ornithine, as well as for amides and secondary amines such as asparagine, glutamine or proline, arginine. The heterocycles such as tryptophan and histidine also give cyclic voltammograms similar to those of alkyl amines.

3.1.3. Category III: Amino acids with hydroxyl groups

The serine shown in Fig. 1C is as remarkable as the ethanolamine discussed by Johnson et al. By combining Mode I and Mode II features, the serine resembles a hypothetical combination of a carbohydrate (i.e. glucose) and simple primary amino acid (i.e. glycine). From a purely practical point of view, this combination of features makes it possible to detect serine and other hydroxyl amino acids (threonine, hydroxylysine, and hydroxyproline) by either the Mode I or Mode II technique. Other types of amino acids will appear with the hydroxyl amino acids in Mode II only, and will remain undetected (suppressed) in Mode I.

3.2. Designing a bi-modal waveform

The possibility of selectively suppressing signals of certain amino acids while maintaining a full

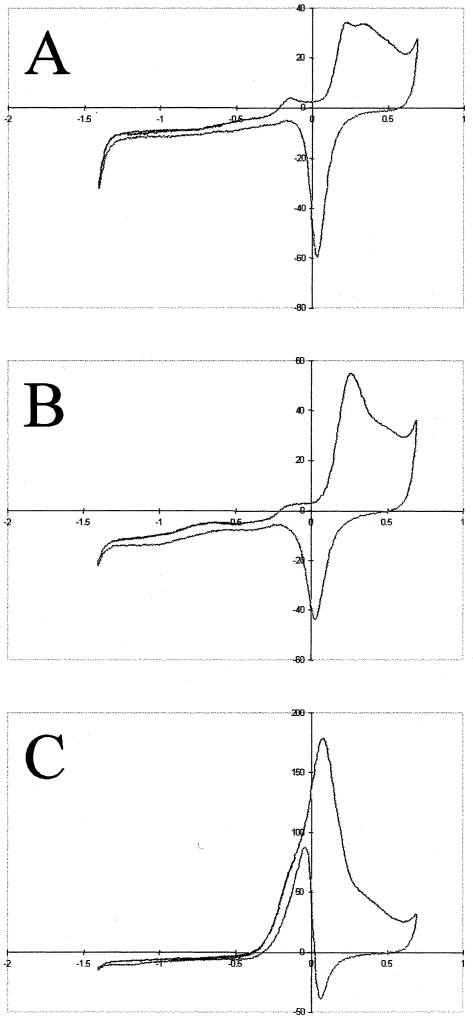

Fig. 1. Rotated disk voltammetry at 900 rpm at gold electrodes. The disk potential was swept between −1.4 and +0.7 at 50 mV/s. The disk current is plotted as a function of disk potential. (A) 1 mM leucine in 100 m*M* sodium hydroxide, (B) 1 m*M* lysine in 100 m*M* sodium hydroxide, (C) 1 m*M* serine in 100 m*M* sodium hydroxide.

sensitivity for carbohydrates and hydroxyl amino acids is of considerable interest whenever complex mixtures of those compounds have to be analyzed. In its present form, the recently introduced amino acid waveform (Fig. 2A) does not lend itself to the Mode I-type of sampling anodic current. For carbohydrates and similar hydroxyl compounds, the anodic oxidation current has to be integrated in the range of −0.05 to +0.05 V vs. Ag/AgCl for at least 100 ms

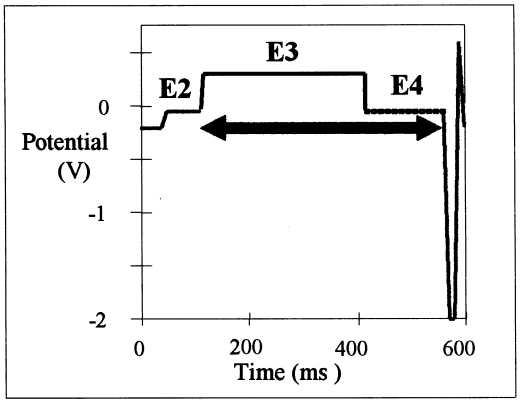

A

Time	Potential	Integration
0	-0.2	
40	-0.2	
50	-0.05	
110	-0.05	Begin
120	0.28	
410	0.28	
420	-0.05	
560	-0.05	End
570	-2	
580	-2	
590	0.6	
600	-0.2	

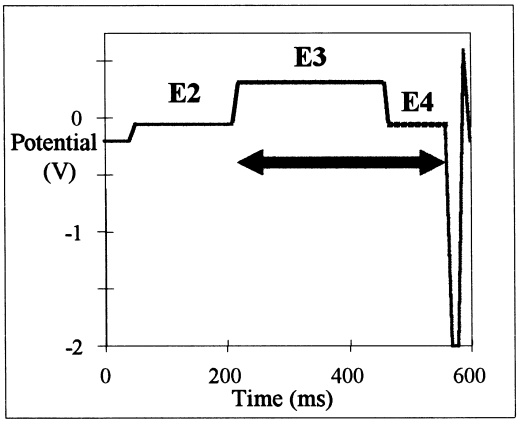

B

Time	Potential	Integration
0	-0.2	
40	-0.2	
50	-0.05	
210	-0.05	Begin
220	0.28	
460	0.28	
470	-0.05	
560	-0.05	End
570	-2	
580	-2	
590	0.6	
600	-0.2	

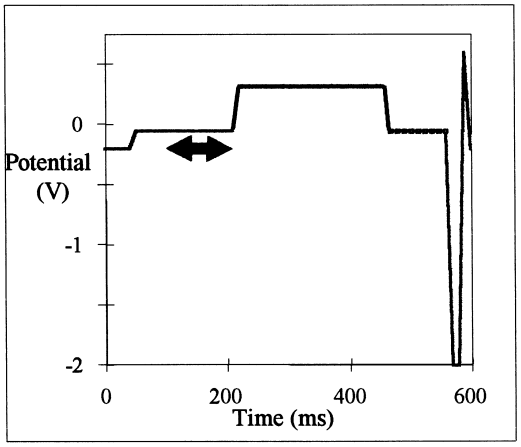

C

Time	Potential	Integration
0	-0.2	
40	-0.2	
50	-0.05	
110	-0.05	Start
210	-0.05	End
220	0.28	
460	0.28	
470	-0.05	
560	-0.05	
570	-2	
580	-2	
590	0.6	
600	-0.2	

Fig. 2. Three detection waveforms. The double arrow indicates a current integration period. The potential values are those vs. Ag/AgCl. If pH electrode is used as a reference, 0.33 V has to be added to all potential values of the waveform. See Ref. [1] for more detailed discussion.

for the method sensitivity to be considered acceptable [4–6]. In that potential range, the waveform in Fig. 2A has just one step (E2) lasting only 60 ms. Increasing the length of the E2 step without reducing the length of another step would expand the total cycle beyond 1.0 s. As explained previously [4], this is undesirable in view of the required data acquisition frequency. We experimented with shortening the duration of the E3, E4 steps while extending that of the E2 step and arrived at the new waveform depicted in Fig. 2B and C. The respective lengths of steps E2 and E3 are 160 and 240 ms. The maximum possible lengths of Mode I and Mode II integration steps are 100 and 350 ms, respectively.

We experimentally verified (results are not shown here) that the Mode II detection sensitivity of the waveform in Fig. 2B remained unchanged. The slopes of the calibration plots (based on four concentrations between 2 and 8 μM) are only 5–15% lower, depending on the individual amino acid. The detection limits, evaluated as multiples of baseline noise, were identical, whether the original (Fig. 2A) or the modified (Fig. 2B) waveforms were utilized.

3.3. Selective detection using the bi-modal waveform

In the initial selectivity evaluation of the bi-modal waveform, we chose three values of E2 (−0.05, 0.00 and +0.05 V vs. Ag/AgCl) to use with both modes of current integration. Identical injections of an amino acid standard were applied. All other potentials were as shown in Fig. 2B and C. The resulting Mode I and Mode II chromatograms (with E2=0.05 V) are presented in Fig. 3. The peak areas corresponding to all six experiments are shown in Table 2, as are the ratios calculated for each pair of Mode I and II chromatograms at one of the three values of the E2 potential. As expected from the voltammetry results (see Fig. 1), there are three categories of analytes in Fig. 3 and Table 2.

With the amounts injected (200 pmol), all the aliphatic, aromatic, and carboxylated analytes are only detected in Mode II. In the Mode I chromatogram, the detection of these analytes is suppressed. Depending on the presence or absence of the gradient sharpening effect and on mobile phase pH, we

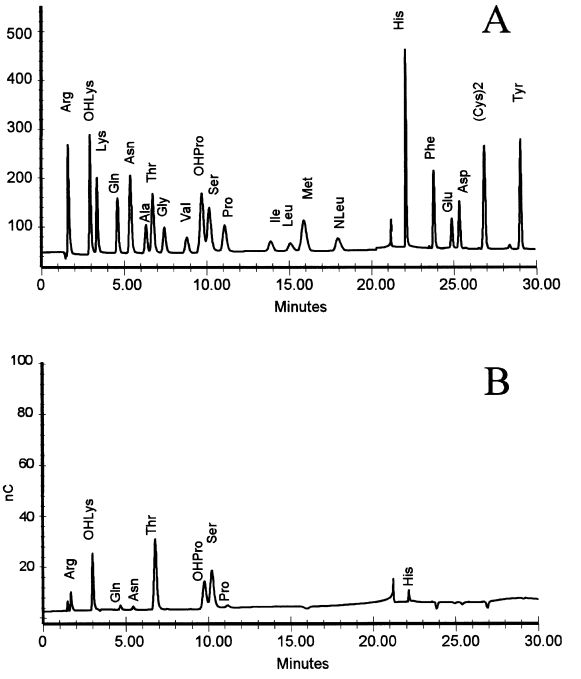

Fig. 3. Amino acid standard separated with Gradient A (see Table 1). All components were at 200 pmol. (Nleu at 313 pmol). (A): Mode II detection, see Fig. 2B waveform with E2=−50 mV. (B): Mode I, see Fig. 2C waveform with E2=50 mV.

observed only several analytes (alanine, glycine, valine). The peak area ratios for this group are >200. At 200 pmol, all basic amino acids can be detected by both modes of current integration. In Table 2, their ratios are in the 30–100 range. The hydroxylated amino acids, amino sugars, and carbohydrates, on the other hand, are easily detected by both detection modes. All their peak area ratios in Table 2 are less than 11.

This observation of three distinct categories of peak areas is potentially useful for separating complex mixtures of amino acids. Thus it is possible, for example, to resolve closely co-eluting peaks providing they belong to different categories of analytes. Furthermore, the peak area ratios can be used to provide additional proof of identity by employing a method similar to the use of UV wavelength ratios in combination with retention times [15]. Finally, based on their peak area ratios, unknown peaks can be

Table 2
Peak areas and peak-area ratios at three different values of E2 (−50, 0 and +50 mV)[a]

AA	Mode						Ratio		
	II	I	II	I	II	I			
mV	−50	−50	0.0	0.0	+50	+50	−50	0.0	+50
Arg	1342	40	1605	32	1576	29	34	50	54
OHLys	1643	151	1656	151	1670	170	11	11	10
Lys	1065	0	1101	0	1168	0	n.a.	n.a.	n.a.
Gln	934	14	948	12	967	14	67	79	69
Asn	1616	11	1704	8	1830	7	147	213	261
Ala	581	2	605	2	626	1	291	303	626
Thr	1376	326	1382	358	1430	377	4	4	4
Gly	630	3	660	3	701	0	210	220	n.a.
Val	447	0	447	1	450	1.2	n.a.	447	375
OHPro	1450	166	1765	228	1626	294	9	8	6
Ser	1520	253	1496	282	1497	294	6	5	5.1
Pro	911	18	844	50	788	98	51	17	8
Ile	348	0	338	0	330	0	n.a.	n.a.	n.a.
Leu	319	0	298	0	308	0	n.a.	n.a.	n.a.
Met	1335	0	1328	0	1365	0	n.a.	n.a.	n.a.
Nleu	541	0	519	0	549	0	n.a.	n.a.	n.a.
His	1960	23	1967	31	2071	53	85	63	39
Phe	1174	0	1215	0	1219	0	n.a.	n.a.	n.a.
Glu	446	0	447	0	437	0	n.a.	n.a.	n.a.
Asp	713	0	763	0	767	0	n.a.	n.a.	n.a.
(Cys)2	1816	0	1877	0	1930	0	n.a.	n.a.	n.a.
Tyr	1595	0	1609	0	1611	0	n.a.	n.a.	n.a.
GalN	1653	247	1670	300	1679	354	7	6	5
GlcN	1812	305	1830	362	1832	411	6	5	4
Glc	1147	200	1211	254	1276	298	6	5	4
Fru	881	123	911	164	980	201	7	6	5

[a] All analytes at 200 pmol (single exception: Nleu 313 pmol).

placed in one of the three main categories. Such a preliminary category assignment along with the information from retention behavior represents a good start toward the final identification of a hitherto unknown sample component.

3.4. Separations of carbohydrates in a mixture with amino acids

The separations on an AminoPac PA10 column are based on interactions with anion-exchange groups and on the dissociation degree of the analytes. Amino acids and carbohydrates exhibit considerably different values of dissociation equilibria. Most amino acids are anionic below pH 10, while the dissociation of most carbohydrates only starts at about pH 11. Correspondingly, adjusting the hydroxide concentration can give differing results for amino acids and carbohydrates.

Fig. 4A shows an overlay of carbohydrate and amino acid separations using Gradient A from Table 1. Glucose and fructose are not resolved from the two amino acids typically present in cell culture samples. Changing to Gradient B, Table 1 (Fig. 4B) does not result in much of an improvement. Glucose, the more important of the two carbohydrates in the context of fermentation monitoring, slides even further below the group of amino acid peaks. Only a minor reduction in hydroxide concentration between Gradients B and C (Fig. 4C) is needed to resolve glucose from the three nearest amino acid peaks.

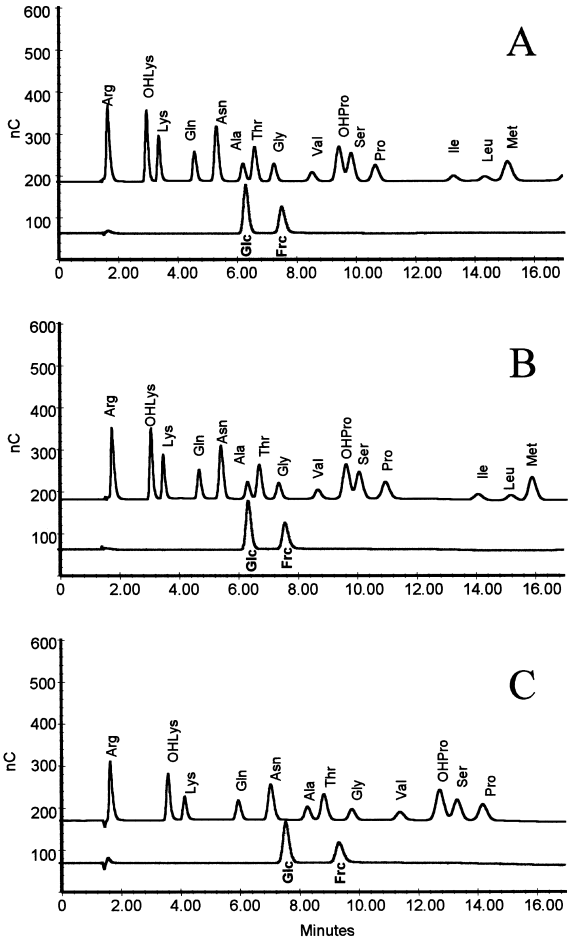

Fig. 4. Optimizing the resolution of alanine and glucose peaks. Note: Each of the three figures is an overlay of two chromatograms obtained under identical conditions. (A) Gradient A, (B) Gradient B, (C) Gradient C. All three gradients are described in Table 1. The chromatograms were detected in Mode II with the waveform from Ref. [4].

However, the peak of fructose still co-elutes with that of glycine.

3.5. Selective detection in fermentation broth and cell culture media

Glucose concentration is a key parameter commonly measured and controlled in both bacterial fermentations and mammalian cell cultures. A wide variety of other media components including amino acids can also play important roles in fermentation behavior and performance. The utility of the bi-modal integration technique was next evaluated for its ability to simultaneously monitor amino acid and sugar compositions in fermentor samples. Typical chromatograms from a recombinant mammalian cell culture medium sample are shown in Fig. 5. Fig. 5A was obtained with Mode II, while the chromatogram in Fig. 5B was generated with the Mode I detection on the same bi-modal waveform (Fig. 2). All three phenomena discussed in connection with Fig. 3 and Table 2 are discernible by comparing the two chromatograms in Fig. 5. The peak size of carbohydrate and hydroxyl amino acids undergoes the smallest change between the two modes of detection, consequently the peaks of glucose, threonine, and serine become more prominent in the Mode I chromatogram. A similar pattern, but to a lesser degree, is also followed by the analytes with additional amine and amide (i.e. glutamine, histidine). Proline, a secondary amine, also belongs to that category. As expected, the peaks belonging to aliphatic amino acids are either strongly reduced (alanine) or have completely disappeared (isoleucine, leucine, and glycine) in the Mode I chromatogram. By eliminating the glycine peak in Mode I, we were able to resolve a peak belonging to fructose that was co-eluting with glycine in the Mode II chromatogram (we did not expect fructose in the sample), thereby enabling us to trace its origin as a trace impurity from glucose.

Additionally, the size reduction of the two peaks eluting between 2–3 min suggests that these peaks are carbohydrates. From the known elution behavior, we were subsequently able to identify one of these compounds as mannitol.

In summary, with our methodology (Fig. 5) we were able to demonstrate the separation and identification of amino acids and sugars in a complex cell growth medium. Comparable chromatograms were obtained from microbial fermentation broths as well (data not shown). By applying the bi-modal integration technique, we were able to investigate the nature of the components in each peak, and could individually quantify an amino acid (glycine) and a sugar (fructose), which co-eluted from the column. These results demonstrate the utility of our technique for simultaneous monitoring a variety of the key components in cell cultures and fermentations. They

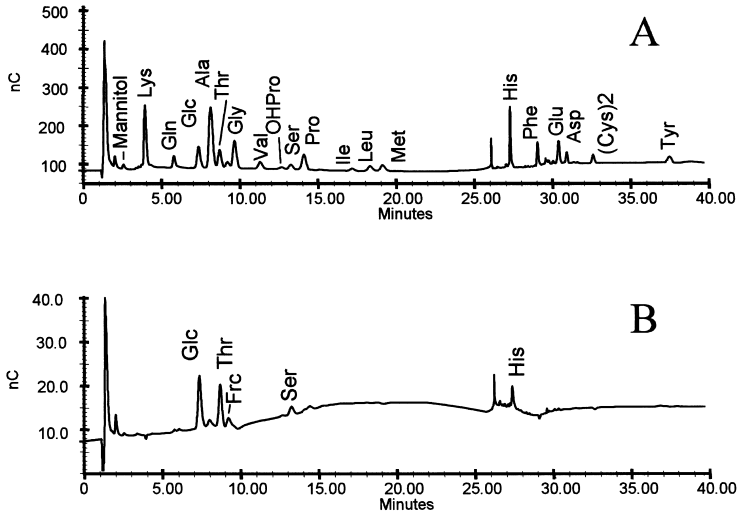

Fig. 5. Fermentation sample separated with Gradient C (see Table 1). Injection: 25.0 μl of a 1:250 diluted sample. Mode II (A) and Mode I (B) waveforms with E2 step at −50 mV vs. Ag/AgCl (+0.28V vs. Glass/3 m KCl/Ag/AgCl).

should also aid in gaining a better understanding of cellular metabolic behavior under fermentor conditions.

References

[1] P.T. Kissinger, C. Refshauge, R. Dreiling, R.N. Adams, Anal. Lett. 6 (1973) 465.
[2] S. Hughes, D.C. Johnson, Anal. Chim. Acta 149 (1983) 1.
[3] W.L. LaCourse, Pulsed Electrochemical Detection, Wiley Interscience, New York, 1997.
[4] A.P. Clarke, P. Jandik, R.D. Rocklin, Y. Liu, N. Avdalovic, Anal. Chem., in press.
[5] D.C. Johnson, W.R. LaCourse, Anal. Chem. 62 (1990) 589A.
[6] D.C. Johnson, D. Dobberpuhl, R. Roberts, P.J. Vandenberg, J. Chromatogr. 640 (1993) 79.
[7] P.J. Vandenberg, J.L. Kowagoe, D.C. Johnson, Anal. Chim. Acta 260 (1992) 1.
[8] P.J. Vandenberg, D.C. Johnson, Anal. Chim. Acta 290 (1994) 317.
[9] A.J. Tudos, P.J. Vandenberg, D.C. Johnson, Anal. Chem. 67 (1995) 552.
[10] J. Evrovski, M. Callaghan, D.E.C. Cole, Clin. Chem. 41 (1995) 757.
[11] W.R. Arathoon, J.R. Birch, Science 232 (1986) 1390.
[12] T.A. Bibila, D.K. Robinson, Biotechnol. Prog. 11 (1995) 1.
[13] W. Zhou, J. Rehm, A. Europa, W.S. Hu, Cytotechnology 24 (1997) 99.
[14] L. Xie, D.I.C. Wang, Biotechnol. Bioeng. 51 (1996) 725.
[15] R.S. Stevenson, in: T.M. Vickrey (Ed.), Liquid Chromatographic Detectors, Marcel Dekker, New York, 1983, p. 32, Ch. 2.